

Examining Sea Ice SAR Signatures in the Arctic

Benjamin Holt
Jet Propulsion Laboratory
California Institute of Technology
Pasadena CA 91109
PH 818-354-5473

Introduction

This research examines the seasonal changes of the sea ice cover in the Arctic Basin as it responds to atmospheric and oceanic conditions. Monitoring this process provides a means of determining the onset and extent of the annual seasonal stages, which is thought to be an indicator for detecting climate change in the polar regions. Much of the response of sea ice to seasonal conditions results in changes in the phase of water (both in the ice and snow cover), surface roughness, and internal properties such as air bubbles. Imagery from SAR has proven to be an important tool for revealing these changes since radar backscatter is affected by both surface roughness and dielectric properties of water and salt. The major ice types and ice features may have unique SAR backscatter signatures because of the inherent variations in, surface roughness, salinity, and internal properties in each category.

The approach being taken is to examine SAR imagery from ERS-1 and JERS-1 to determine the variations in SAR signatures by season and region in the Arctic Basin and to evaluate the capability of the ASF classification algorithm to monitor these changes (Kwok et al., 1992). The procedure involves extracting signatures from time series of SAR imagery and determining the sensitivity of the signatures to changes in the condition of the ice as it responds to surface air temperatures. Regional comparisons are also made. The evaluation of the ice classification algorithm is done by comparing sea ice field measurements with ice type maps.

Results

Late summer and fall freeze-up. Examination of ERS-1 SAR sea ice signatures from August through October, 1991 in the Beaufort and Chukchi Seas has been performed (Holt et al., 1993). In the summer period multiyear and first year ice have similar (low) SAR signatures due to uniform wetting of the ice surface and therefore cannot be separated in the radar data (Figure 1). There are large variations in the signatures of the thick ice related to air temperature excursions above and below freezing as the ice surface either is rapidly freezing or thawing (Figure 2). These signature variations provide a direct estimate of when the ice surface is undergoing ablation (Figure 3). When temperatures remain steadily below freezing in the fall, the signatures of multiyear ice also become quite stable at a high value that continues into the winter months (Figure 1). Newly-formed and younger first year ice is also distinct (dark) from multiyear ice. Thus variations in the late summer melt period and the start of ice growth are clearly identifiable in the ERS-1 imagery.

Validation of sea ice classification products during winter Sea ice and snow measurements were obtained coincidentally to ERS-1 SAR acquisitions during the Lead Experiment in the Beaufort Sea that took place in March/April 1992. These measurements included ice type, thickness, salinity, temperature, roughness, internal properties, and snow thickness, density, and temperature. Also obtained were surface scatterometer measurements of several different ice types. Extensive observations were made of new ice growth in leads. Regional observations and measurements were obtained from helicopter and snow machine. These measurements have been used to validate the winter ice type products generated by the ASF ice classification algorithm.

Comparisons of identified ice types were made directly with the ice classification data. Results show that multiyear ice is accurately classified with small errors arising from highly

deformed first year ice and wind-roughened open water, generally accounting for a small fraction of the ice cover, which may have signatures similar to multiyear ice. Smooth and deformed first year ice (over 30 cm in thickness) as well as new ice/calm open water have distinct signatures and are largely accurately classified, however, it has been found that significant errors may occur in each of these three classes for several reasons. For first year ice, there is a wide variation in signatures, so the demarcation between rough and smooth is not distinct. During high winds, open water can be very bright and hence may be incorrectly identified as first year or even multiyear ice, as mentioned above. Most importantly, new ice in leads undergoes rapid and dramatic changes in signatures during growth and is subject to deformation, which results in a wide variation of signatures that overlaps with first year signatures. Thus some new and young ice forms in leads may be incorrectly classified as smooth or rough first year ice. The overall error in the ASF ice classification maps using ERS-1 SAR imagery is probably about 5% but this value awaits quantitative confirmation.

References

Holt, B., G. Cunningham, and R. Kwok, Sea ice radar signatures from ERS-1 SAR during later summer and fall in the Beaufort and Chukchi Seas, Proceedings First ERS-1 Symposium, Cannes, Nov. 4-6, 1992, ESA SP-359, 339-342, 1993.

Kwok, R., E. Rignot, B. Holt, and R. Onstott, Identification of sea ice types in spaceborne SAR data, *J. Geophys. Res.*, 90(C3), pp. 5035-5044, 1992.

Figure Captions

1. ERS-1 SAR signatures of multiyear ice in the Beaufort and Chukchi Seas in 1991 by day of year. The variations in signatures from day to day (before day 250) are due to air temperature fluctuations above and below 0°C. In some cases the range of signatures on a particular day are due to warming on the lower latitudes while the northerly latitudes remain cold.

2. ERS-1 SAR signatures of multiyear ice in the Beaufort and Chukchi Sea in 1991 compared with air temperature. Note that there is little change in the signatures once air temperatures fall steadily below freezing.

3. Summer ERS-1 SAR images in the Beaufort Sea over a short time period where the signatures vary with temperature fluctuations above and below freezing, indicating that the ice surface is either wet or frozen. This information provides a direct estimate of when top surface ablation is occurring.

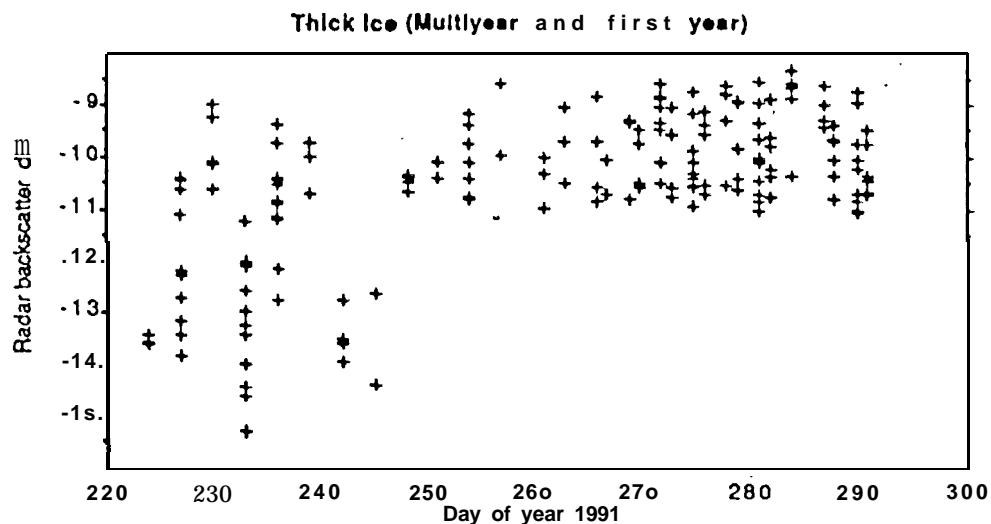


Fig. 1

Figure 2

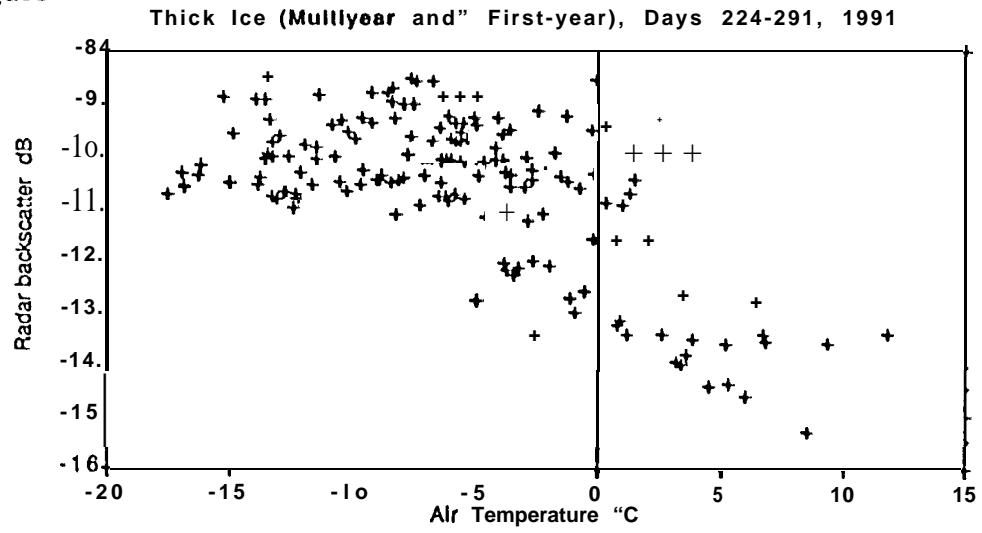
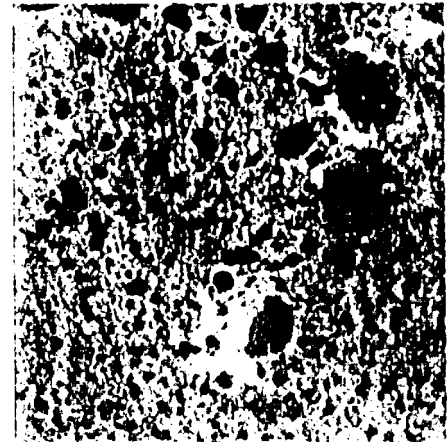


Figure 3



ORBIT 462 AUG 18, 1991
LAT 73.1° N LON 159.1° W



ORBIT 505 AUG 21, 1991
LAT 73.10° N LON 159.0° W



ORBIT 548 AUG 24, 1991
LAT 73.3° N LON 159.3° W

